ASIAN JOURNAL OF PHARMACEUTICAL AND CLINICAL RESEARCH

INNOVARE ACADEMIC SCIENCES
Knowledge to Innovation

Vol 18, Issue 5, 2025

Online - 2455-3891
Print - 0974-2441

Research Article

PREPARATION AND EVALUATION OF VORICONAZOLE HYDROGEL USING CYCLODEXTRIN-BASED NANO SPONGES

MD APSAR PASHA*, SEEMA TOMAR

Faculty of Pharmaceutical Sciences, Motherhood University, Roorkee, Uttarakhand, India.
***Corresponding author: Md Apsar Pasha; Email: farhanpharma2@gmail.com**

Received: 24 February 2025, Revised and Accepted: 09 April 2025

ABSTRACT

Objective: This project aimed to develop a cyclodextrin-based nanosponge (CDNS) gel for topical skin application to enhance the therapeutic efficacy, distribution, and stability of voriconazole (VO). The focus was on improving drug release, skin penetration, and antifungal activity while preventing VO's photodegradation and chemical degradation.

Methods: CDNS was prepared by crosslinking cyclodextrins with diphenyl carbonate using convection heating. VO-loaded nanosponges (VONS) were freeze-dried and incorporated into a hydrogel formulation with Carbopol 974, propylene glycol, and ethanol, optimized through Box-Behnken design. Procedural parameters and quality attributes were analyzed using statistical tools like analysis of variance. The formulation was characterized by Fourier transform infrared spectroscopy (FTIR), differential scanning calorimetry (DSC), and X-ray diffraction (XRD) to confirm the inclusion complex formation. Particle size, polydispersity index, zeta potential, and encapsulation efficiency were evaluated. Transmission electron microscopy (TEM) was used to assess the nanosponges' morphology.

Results: Optimized VONS exhibited particle sizes of 50–75 nm with minimal polydispersity, ensuring uniform distribution. High zeta potential values confirmed stability and low agglomeration. FTIR, DSC, and XRD confirmed the formation of inclusion complexes, while TEM revealed spherical nanoparticles. The encapsulation efficiency was high, enhancing drug loading. *In vitro* studies showed faster drug release from VONS compared to pure VO. Topical hydrogels (VONS2, VONS8, and VONS12) exhibited controlled drug release and superior skin penetration over 12 h. The formulation prevented VO photodegradation and chemical degradation for up to 6 months, with significant improvements in antifungal efficacy and stability.

Conclusion: The developed CDNS gel demonstrated controlled drug release, enhanced skin penetration, and superior storage stability, making it a promising strategy for improving VO's therapeutic impact in topical applications. The formulation successfully addressed challenges like photodegradation, chemical degradation, and low skin permeability.

Keywords: Voriconazole, Box-Behnken design, Nanosponges, Freeze drying, Inclusion complex, Skin permeability.

 DOI: http://dx.doi.org/10.22159/ajpcr.2025v18i5.54060. Journal homepage: https://innovareacademics.in/journals/index.php/ajpcr

INTRODUCTION

Voriconazole (VO) is a synthetic triazole antifungal agent that inhibits ergosterol synthesis, a critical component of fungal cell membranes, leading to cell death. This occurs through the drug's binding to lanosterol 14-alpha-demethylase, an enzyme responsible for converting lanosterol to ergosterol in fungal cells. The reduced ergosterol levels and the accumulation of 14-alpha-methyl sterols disrupt the fungal membrane. VO specifically targets fungal cells, making it both safe and effective without affecting mammalian cells [1,2]. It is commonly used for treating invasive aspergillosis, candidemia, and esophageal candidiasis thorugh oral and intravenous administration. As a first-line treatment for invasive aspergillosis, VO is considered as effective as amphotericin B [3].

A significant challenge with standard VO formulations is the variable and unpredictable pharmacokinetics. Factors such as diet, stomach pH, and concomitant medications can influence VO's oral bioavailability, causing substantial variation in drug exposure across patients. The intravenous form may lead to side effects such as fever, rash, and elevated liver enzymes, necessitating close monitoring. The limited solubility and stability of conventional formulations hinder their bioavailability and therapeutic effectiveness. Since VO has low water solubility and a poor dissolution rate, its stability, especially in acidic environments, is compromised, reducing its therapeutic potential [4-6]. To address these limitations, novel formulations and delivery technologies for VO are being developed, including lipid-based and cyclodextrin (CD)-based formulations, nanocrystals, and prodrugs. These innovations enhance solubility, stability, and bioavailability, mitigate side effects, and reduce dosing frequency, potentially overcoming the restrictions of traditional delivery methods [7-11].

Several studies have explored the use of CD to improve VO's solubility and bioavailability. Common CD derivatives such as hydroxypropyl-β-CD (HP-β-CD) and sulfobutyl ether-β-CD (SBE-β-CD) are widely utilized in VO formulations. CD-based VO systems can enhance solubility, stability, and bioavailability, thus expanding its use in treating fungal infections [12,13]. CD-based nanosponge (CDNS) also show promise in VO formulation research. These three-dimensional, cross-linked structures form stable inclusion complexes with hydrophobic drugs like VO. By encapsulating VO in CDNS, it is possible to improve solubility, stability, and bioavailability [14].

Hydrogels are crosslinked polymeric networks capable of absorbing large amounts of water and swelling into gels. Combining CDNS with hydrogels can create a new drug delivery system. The sustained release and targeting capabilities of CDNS, combined with the swelling and mechanical properties of hydrogels, allow for the development of a system that delivers drugs in a controlled and prolonged manner. In addition, hydrogels can be designed to release the drug in response to specific stimuli, such as pH, temperature, or enzyme activity, further enhancing drug delivery. Together, CDNS and hydrogels form a multimodal drug delivery system that improves solubility, stability, bioavailability, and enables sustained, targeted release [15-17].

To optimize these drug delivery systems, pharmaceutical researchers often employ response surface methodology (RSM), a robust statistical technique used to explore the interactions between variables and their effects on outcomes. RSM simplifies formulation development by identifying critical parameters of CDNS and making optimization processes more feasible [18,19]. The Box-Behnken experimental design within RSM is particularly useful for evaluating the impact of multiple independent factors on the outcome while minimizing the number of experimental runs, making it an ideal tool for pharmaceutical and nanotechnology process optimization [20,21]. This project aims to develop a hydrogel-based VO delivery system incorporating CDNS for sustained, targeted drug release, ultimately improving bioavailability and therapeutic efficacy.

MATERIALS AND METHODS

Materials

As previously mentioned, our team developed CDNS (NS1-NS15). VO was provided as a gift sample by Hetero Laboratories in Hyderabad. Carbopol 934, propylene glycol, triethanolamine, and N-methyl-2-pyrrolidone were sourced from S.D. Fine Chem in Mumbai. All other chemicals and reagents used were of analytical grade. Milli Q water (Millipore) was used in the studies.

Methods

Preparation of CDNS using different CD

To prepare 15 variations of CDNS, β-CD, 2-HP β-CD, and SBE-β-CD were combined with diphenyl carbonate as a cross-linking agent and dissolved in dimethyl formamide. The mixture was refluxed at 90°C in an oil bath (Labline, Oil Bath) with continuous stirring for 6 h, followed by rinsing with water and filtration. After grinding, the resulting fine powder was dispersed in water, and the colloidal component was lyophilized (LARK INDIA). The vacuum-dried nanosponges were stored at 25°C for later use. Characterization of the nanosponges included particle size distribution, Zeta Potential (ZP; Master sizer 2,000, Malvern, UK), Fourier transform infrared spectroscopy (FTIR) (Master sizer 2,000, Malvern, UK), differential scanning calorimetry (DSC) (Perkin Elmer STA 8,000 Thermal Analyzer), XRPD (Philips X-ray diffractometer, PW-1710), and solubility efficiency analyses.

Preparation of VO-loaded nanosponges (VONS)

A freeze-dried drug-loaded NS was prepared [14]. The precisely weighed NS was suspended in 50 mL of Milli Q water and stirred with a magnetic stirrer (2MLH, Remi, Mumbai, India). The excess drug was then added, followed by sonication (Vibra cell VCX 750, Sonics and Materials, Inc., USA) for 10 min and continuous stirring for 24 h. After centrifuging at 2,000 rpm for 10 min (Sigma 3–30 KS, Sigma Labor Centrifuge, Germany), the uncomplexed drug formed a deposit beneath the colloidal supernatant. The supernatant was then freeze-dried at −20°C and 13.33 mbar using a LARK INDIA lyophilizer. The resulting powder was stored in a desiccator.

Physico-chemical characterization of VONS

VONS were analyzed for their EE, percent drug loading in NS, Particle Size, PDI, ZP, transmission electron microscopy (JEM 2100, JOEL, Tokyo, Japan), FTIR, DSC, XRPD, and *in vitro* release of Drug from NS formulations [22].

Preparation of hydrogel formulation of VONS

VONS gel was formulated using Carbopol 974 [15]. To prepare the gel, Carbopol 974 polymer was gradually dispersed into a specified volume of water while stirring continuously. Methylparaben sodium (0.01%, w/v) and propylparaben sodium (0.1%) were then added, and the mixture was allowed to soak for 24 h. The dispersion was then hydrated and swollen for 60 min. Afterward, the drug (0.1%, w/w) was incorporated into a mixture of propylene glycol, ethanol, and 10% of 3-Carene (an optimized permeability enhancer), with continuous stirring. This mixture was transferred into the pre-soaked Carbopol and stirred for 20 min. Triethanolamine was added to the dispersion and stirred until a clear, viscous, homogenous gel was formed, with a pH range of 6.0–7.0 for optimal performance. The formulation of VONS was optimized using Box-Behnken design (BBD) with Carbopol 974 (1–3%, w/w), propylene glycol (5–10%), and ethanol (10–20%), and statistical screening was used to fine-tune the formulation.

Design of experiments

The formulations were optimized using Design Expert®, employing second-order polynomial models and quadratic response surfaces within a 3-factor, 3-level BBD. The independent and dependent variables, along with their low, medium, and high coded values, are presented in Table 1. The experimental design resulted in the following polynomial equation:

$$Y_0 = B_0 + B_1X_1 + B_2X_2 + B_3X_3 + B_{12}X_1X_2 + B_{13}X_1X_3 + B_{23}X_2X_3 + B_{11}X_1^2 + B_{33}X_2^2 + B_{33}X_3^2 \quad (1)$$

Y0 represents the dependent variable, while B0 denotes the intercept. The regression coefficients, B1, B2, and B3, are determined from the experimental values of Y. The coded independent variables are X1, X2, and X3. The interaction terms include X1X2, X1X3, and X2X3, and the quadratic terms consist of $X1^2$, $X2^2$, and $X3^2$

Numerical optimization

The optimal values for the independent variables were established through numerical optimization, considering response characteristics and influencing factors. Subsequently, the nanosuspension formulation was prepared in triplicate under the optimized conditions to validate the optimization process.

Evaluation of gel formulations

pH (pHCal, Analab Scientific Instruments Private Limited, Vadodara, India) and viscosity (AMETEK Brookfield Visometer) measurements were conducted for the gel formulations. Following the approach outlined by Krabicová *et al*. [16], *ex vivo* permeation studies were carried out on male Wistar rats, and a skin irritation test was performed on the hydrogel. *In vitro* and *in vivo* skin permeation and deposition investigations were based on references [23]. An additional *in vivo* permeation study was carried out on mice [24]. The *in vitro* antifungal activity of NS-encapsulated drug formulations was assessed against *Candida albicans* and *Aspergillus fumigatus*. Stability studies were conducted on carbopol gel formulations, both with free and NS-encapsulated drugs (1%, w/w). All experiments were stored in sealed amber glass containers at ambient temperature (25±2°C/60% RH ±5% RH) under dark conditions. Each experiment was repeated 3 times. Statistical analysis was performed using Statistical Package for the Social Sciences 12.0, and a significance level of $p \leq 0.05$ was considered to indicate statistical significance for the data presented as mean±standard deviation.

Table 1: Variables with coded values in BBD

Independent variables	Coded levels		
	Low (−1)	Intermediate (0)	High (+1)
X_1-Carbopol 974 (% w/w)	1	2	3
X_2-Propylene glycol (% w/w)	5	7.5	10
X_3-Ethanol (% w/w)	10	15	20
Independent variables	**Constraints**		
Y_1-pH of the gel	$4 \leq Y_1 \geq 6$		
Y_2-Viscosity of the gel (cP)	$3,000 \leq Y_2 \geq 3,500$		
Y_3-Flux of the drug (μg/cm²/h)	$90 \leq Y_3 \geq 120$		

BBD: Box-Behnken design

RESULTS AND DISCUSSION

The solubilization efficiency of all 15 VONS was evaluated and compared to free VO in distilled water. All NS (NS1-NS15) enhanced solubility, with NS2 (β-CD: DPC in a 1:4 ratio), NS8 (2-HP β-CD: DPC in a 1:6 ratio), and NS12 (SB-β-CD: DPC in a 1:4 ratio) showing higher solubilization efficiency than plain VO (593.46 µg/mL). The improved solubilization capability of NS could be attributed to drug inclusion complexes and matrix entrapment. The study demonstrated that NS formulations enhance solubilization efficiency, with higher solubilization observed in NS made from SB-β-CD (NS11-NS15) compared to those made from β-CD or 2-HP-β-CD (NS1-NS3). The superior solubilization ability of SB-β-CDNS is linked to its unique properties. The addition of sulfobutyl groups to the β-CD structure enhances its water solubility and complexation capacity. The hydrophilic nature of SB-β-CDNS facilitates better interaction with hydrophobic drugs like VO, improving solubilization. Structural modifications in SB-β-CD may also increase cavity size or alter molecular organization, creating a more favorable environment for drug incorporation. These factors contribute to the superior solubilization capacity of SB-β-CDNS compared to other CD-based NS.

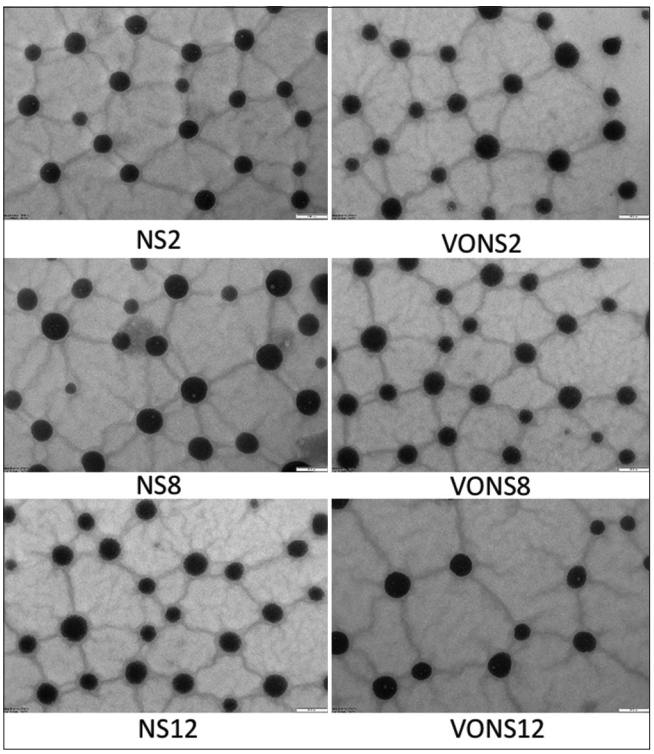

Fig. 1: Transmission electron microscopy images of cross-lined cyclodextrin-based nanosponge and drug-loaded nanosponges

VO was loaded into three types of NS using freeze-drying, and the resulting drug-loaded formulations were named VONS2, VONS8, and VONS12 based on the NS used. All formulations were fine, flowable powders. To determine the drug amount associated with the NS and calculate the drug-to-carrier weight ratio, the average VO payload per gram of lyophilized powder was found to be 367.57 mg across all batches. The high encapsulation efficiency (79.34±3.49%) of VO indicates successful inclusion complex formation. The encapsulation of VO was more efficient in NS12 than in NS7 and NS3.

Morphology and sizes of the VONS

NS and NS complexes scatter laser light within the range of 50–75 nm, exhibiting minimal polydispersity, which suggests a narrow, unimodal particle size distribution. The high ZP values (−24.3±1.16 to −26.8±2.08) contribute to the stability of the complexes, preventing agglomeration. The PDIs are narrow (ranging from 0.06±0.005 to 0.23±0.005) in homogeneous colloidal solutions. Each formulation was found to be a fine, free-flowing powder. As shown in Fig. 1, drug-loaded NS maintains a spherical shape.

The FTIR spectra of VONS complexes (VONS2, VONS8, VONS12) are displayed in Fig. 2. The FTIR spectrum of VO exhibits prominent C-N, C-F, and C-C stretching bands at 3197.8–3047.3, 1498.6–1454.2, and 1589.2–1454.2 cm^{-1}. The FTIR spectra of plain NS show a carbonate bond peak at 1,780 cm^{-1}, C-H stretching and bending vibrations at 2,918 and 1,418 cm^{-1}, and the primary alcohol's C-O stretching vibration at 1,026 cm^{-1}. The FTIR spectra of NS formulations only reveal peaks associated with the NS, with no drug-related peaks, indicating efficient encapsulation of VO.

The DSC thermogram of VO shows an endothermic peak at 130°C, corresponding to its melting point. The DSC thermograms of NS (Fig. 2) show an exothermic peak around 350°C. The VONS complexes exhibit only NS-related peaks, and the freeze-drying process eliminates the drug's endothermic peak. The absence of this peak suggests interactions between the formulation components, which may lead to the drug's amorphous state or the formation of inclusion complexes. The removal of the endothermic peak indicates a change in the physical state of the VO within the NS complex.

X-ray diffraction (XRD) patterns of pure VO, CD, and VONS were examined to assess their physical properties. VO exhibits distinct crystalline peaks, as shown in Fig. 2. However, the NS complexes do not show the characteristic peaks of pure VO, indicating the successful incorporation of the drug into the NS. The absence of crystalline peaks in

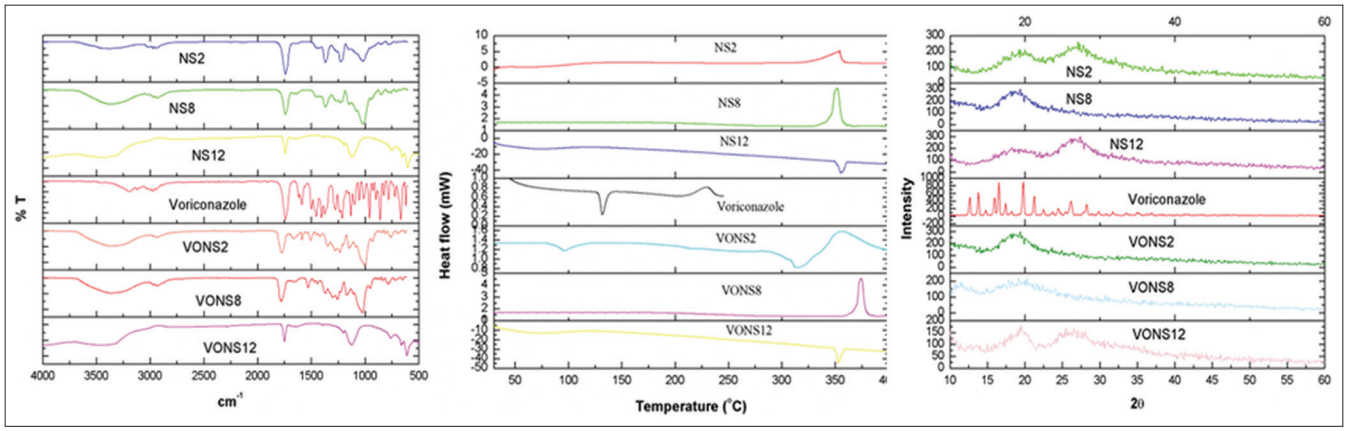

Fig. 2: Fourier transform infrared spectroscopy, differential scanning calorimetry, and X-ray diffraction spectra of cross-lined cyclodextrin-based nanosponge and drug-loaded nanosponges

the NS complexes suggests that the VO is incorporated in an amorphous state within the matrix. The FTIR, DSC, and XRD results support the conclusion that the NS formed an inclusion complex with VO.

In simulated gastric medium, both VO and VONS dissolved, with NS releasing VO at a faster rate than pure VO (11.1%) after 24 h. After 2 h, the release of the drug from NS complexes exceeded 30%. Over time, NS formulations released more VO than the control, reaching over 90% in 24 h, highlighting their sustained and enhanced release capabilities. This indicates that VO in NS can improve drug release and control, positioning them as promising candidates for optimizing drug delivery systems.

Various NS were used to create the Carbopol-based VO topical formulation. The drug-loaded NS formulations were referred to as VONS gel, depending on the NS used. For the topical formulation, key quality attributes included pH (Y1), viscosity (Y2), and drug flux (Y3). Critical process parameters were the compositions of Carbopol 974 (A: X1), Propylene glycol (B: X2), and Ethanol (C: X3). These crucial process parameters were optimized using experimental design techniques. A definitive screening design was applied, with thirteen experiments being randomly assigned, and response surface methods were used to analyze the data. Table 2 presents a summary of the design model. All models were significant, with large F-values and multiple linear regression analysis generated polynomial equations for all critical quality attributes. Table 3 displays the mean, standard deviation, R^2, Adjusted R^2, Predicted R^2, Adeq Precision, and % CV of all models.

pH of the gel (Y1)

Physicochemical pH plays a crucial role in regulating metabolic, molecular, and cellular activities. For topical treatments, achieving the optimal pH and buffer capacity is essential to preserve the active ingredients and excipients. Moreover, it can enhance the absorption of non-ionized species of acidic and basic drugs. Controlling pH in formulations enhances stability and efficacy, thereby improving the overall product performance [25]. The experimental findings demonstrate a predictive model for the gel formulation's pH based on the contents of Carbopol 974, Propylene glycol, and Ethanol. In most instances, the model accurately predicts the pH values, with minimal residuals, although occasional variances suggest variability or unaccounted factors. The model appears unbiased, with both positive and negative residuals. For a thorough evaluation of reliability and applicability, it is important to assess the model's significance and the sources of variation. The simplified quadratic model for gel pH displayed

Table 2: Statistical analysis of all response models

Source	Sum of squares	Degrees of freedom	Mean square values	F-value	p-value	Statistical Significance
ANOVA of the reduced quadratic model - pH of the gel						
Model	6.89	9	0.7651	150.86	<0.0001	Significant
A: X_1	5.28	1	5.28	1041.37	<0.0001	
B: X_2	0.5512	1	0.5512	108.70	<0.0001	
C: X_3	0.6050	1	0.6050	119.30	<0.0001	
AC	0.0400	1	0.0400	7.89	0.0262	
A^2	0.3727	1	0.3727	73.48	<0.0001	
Residual	0.0355	7	0.0051			
Lack of Fit	0.0075	3	0.0025	0.3571	0.7880	Not significant
Pure error	0.0280	4	0.0070			
Cor total	6.92	16				
ANOVA of the reduced quadratic model - viscosity of the gel						
Model	8.863×10^6	9	9.848×10^5	486.97	<0.0001	Significant
A: X_1	8.490×10^6	1	8.490×10^6	4198.39	<0.0001	
B: X_2	80844.22	1	80844.22	39.98	0.0004	
C: X_3	79295.56	1	79295.56	39.21	0.0004	
AC	15761.55	1	15761.55	7.79	0.0268	
BC	39513.49	1	39513.49	19.54	0.0031	
A^2	1.353×10^5	1	1.353×10^5	66.91	<0.0001	
B^2	20399.69	1	20399.69	10.09	0.0156	
Residual	14156.06	7	2022.29			
Lack of Fit	4760.24	3	1586.75	0.6755	0.6109	Not significant
Pure error	9395.82	4	2348.96			
Cor total	8.877×10^6	16				
ANOVA of the reduced quadratic model - flux of the drug						
Model	4522.33	9	502.48	147.76	<0.0001	Significant
A: X_1	1819.25	1	1819.25	534.96	<0.0001	
B: X_2	2312.68	1	2312.68	680.06	<0.0001	
C: X_3	56.60	1	56.60	16.64	0.0047	
AB	64.96	1	64.96	19.10	0.0033	
B^2	138.94	1	138.94	40.86	0.0004	
C^2	123.03	1	123.03	36.18	0.0005	
Residual	23.80	7	3.40			
Lack of Fit	1.32	3	0.4413	0.0785	0.9683	Not significant
Pure error	22.48	4	5.62			
Cor total	4546.13	16				

ANOVA: Analysis of variance

Table 3: The model fit statistics of all the responses

S. no.	Response variable	Mean	Standard deviation	R^2	Adjusted R^2	Predicted R^2	Adeq precision	% CV
1	Y_1	5.54	0.0712	0.9949	0.9883	0.9763	41.4236	1.29
2	Y_2	3579.46	44.97	0.9984	0.9964	0.9898	66.5579	1.26
3	Y_3	106.49	1.84	0.9948	0.9880	0.9876	45.3668	1.73

a significant analysis of variance (ANOVA) result (F-value=150.86, p<0.0001), indicating a strong fit to the data. This model includes linear (A, B, C), interaction (AC), and quadratic (A^2) factors. All terms, with F-values and p-values below 0.05, significantly contribute to the model. A p=0.36 for the Lack of Fit test confirms its non-significance relative to pure error, affirming the model's adequacy. The close alignment between Predicted R^2 (0.9763) and Adjusted R^2 (0.9883), with a difference of <0.2, further establishes the model's reliability. Fig. 3a illustrates how the experimental results align with the predictions. With a signal-to-noise ratio of 41.424, the Adeq Precision indicates the model's capability to guide design space exploration. Fig. 3b presents the perturbation plot, highlighting the influence of individual variables on Y1. The equation reveals that A and B negatively affect Y1, while C has a positive impact. At higher levels, A exhibits a quadratic effect on Y1. Three-dimensional response surface and contour plots demonstrate the interaction between variables A and C (Fig. 3c and d).

Viscosity of the gel (Y2)

Viscosity plays a critical role in the performance and effectiveness of topical formulations. It influences the ease of distribution, application, and, most importantly, the release of active ingredients. The release of the drug in topical formulations is directly impacted by the viscosity of the gel. Higher viscosity gels tend to be thicker and more uniform, which can affect their residence time on the skin. This, in turn, influences the absorption and penetration of active ingredients into the skin layers. Consistent viscosity ensures uniform application, enhances patient compliance, and maximizes the therapeutic effect of the formulation. Therefore, understanding and controlling the viscosity of gels is vital in the development of efficient and reliable topical products [26]. The viscosity values of each experimental run were compared to the predicted values from the model, with the residuals presented. The model accurately predicted the gel viscosity, although some differences were observed, indicating that further refinement of the model may be needed.

The ANOVA of the reduced quadratic model for gel viscosity shows a significant F-value of 486.97 and a very low p-value (<0.0001), confirming the model's ability to explain the variability in gel viscosity. Several factors and interactions, including A: X1, B: X2, C: X3, AC, BC, A^2, and B^2, have significant effects on the response variable, as indicated by their low p-values. These factors determine the viscosity of the gel formulation. With a p=0.68 for the lack of fit F-value, the difference between the model and actual data, the non-significant result suggests that the model fits the data well, attributing any unexplained variability to random factors. The Predicted R^2 value of 0.9898 closely matches the Adjusted R^2 of 0.9964, with a difference of <0.2, supporting the model's robustness. Fig. 4a demonstrates the close relationship between observed and predicted values, further confirming the model's accuracy. The Adeq Precision signal-to-noise ratio of 66.558 exceeds the required threshold of 4, verifying the model's suitability for guiding design space exploration. The perturbation plot in Fig. 4b illustrates the effect of each variable on Y2. The equation shows that A and B have a positive influence on Y2, while C has a negative impact. At higher levels, A and C exert a quadratic effect on Y2. Three-dimensional response surface and contour plots in Fig. 4c-f reveal the interactive effects between the variables A and C, as well as between B and C.

Flux of the drug (Y3)

Optimizing the drug flow in topical gel formulations requires careful adjustments to various parameters. Selecting a drug with suitable solubility and dissolution rate, fine-tuning the type and concentration of polymers, incorporating surfactants or penetration enhancers, adjusting pH levels, and managing co-solvent concentrations are crucial factors. Temperature, gel microstructure, and storage conditions also play a significant role. The formulation process is refined through both *in vitro* and *in vivo* evaluations, alongside statistical optimization methods such as Design of Experiments [27,28].

Table 3 presents the optimization results for drug flux in the topical gel formulation. It compares the actual and predicted drug flux values (μg/cm^2/h), along with the residuals. Different concentrations of Carbopol 974 (Factor 1), propylene glycol (Factor 2), and ethanol were tested. Drug flux is the key target in the optimized formulation, and the residuals help assess the predictive model's accuracy by highlighting the difference between observed and predicted values.

ANOVA on the reduced quadratic model for drug flow in the topical gel formulation indicates highly significant results. The model shows

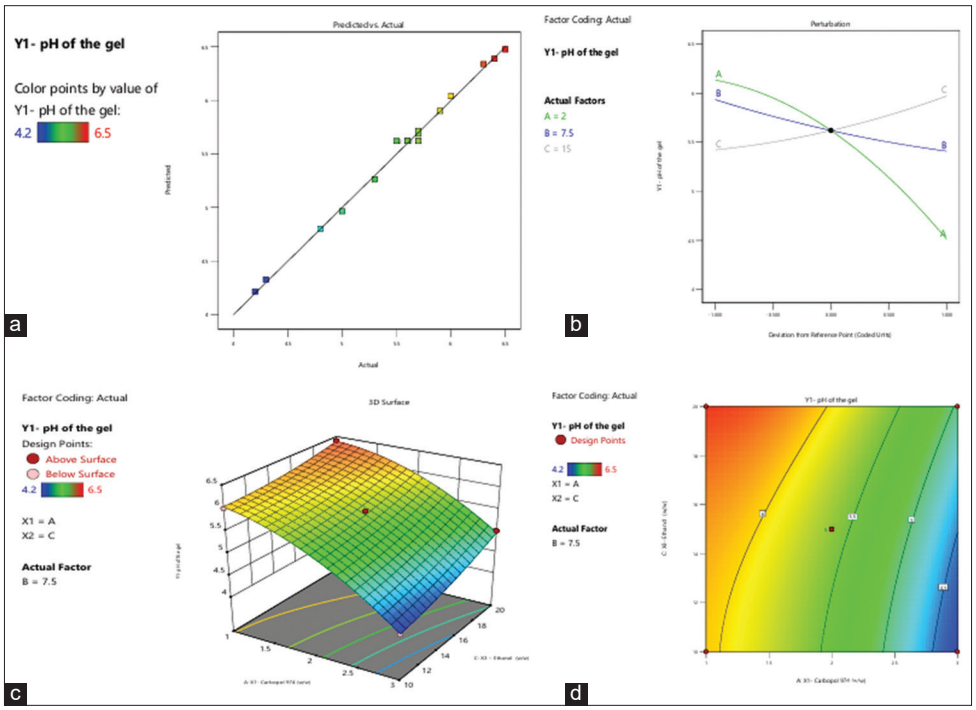

Fig. 3: (a) Predicted versus actual values of the response pH of the gel (b) Perturbation plot displaying the individual influence of variables on Y1 (c and d) 3-D response surface methodology and contour plot displaying the interactive influence of A and C on Y1

a large F-value of 147.76 and a very low p-value (<0.0001), confirming its importance in explaining drug flow variability. Key individual and interaction factors – A: X1, B: X2, C: X3, AB, B^2, and C^2 – have significant effects on the response variable, as evidenced by their low p-values. These parameters and interactions dictate the drug flow in the gel formulation. The lack of fit F-value of 0.08, with a p=0.9683, suggests that the model fits the data well, and any unexplained variability is due to random factors. The model's suitability for optimizing topical gel drug flow is further validated by the close agreement between the Predicted R^2 (0.9876) and Adjusted R^2 (0.9880), with a difference of <0.2. Fig. 5a illustrates the close relationship between observed and predicted values. The Adeq Precision's signal-to-noise ratio of 45.367

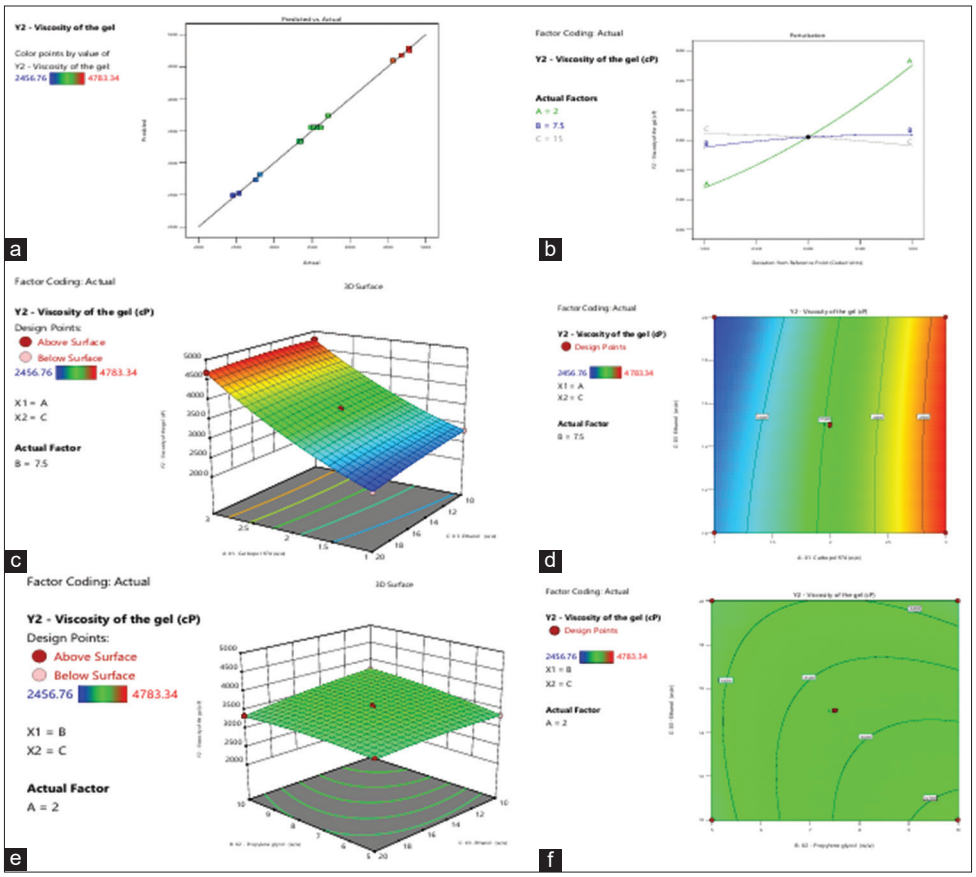

Fig. 4: (a) Predicted versus actual values of the response viscosity of the gel (b) Perturbation plot displaying the individual influence of variables on Y2 (c and d) 3-D response surface methodology (RSM) and contour plot displaying the interactive influence of A and C on Y2 (e and f) 3-D RSM and contour plot displaying the interactive influence of B and C on Y2

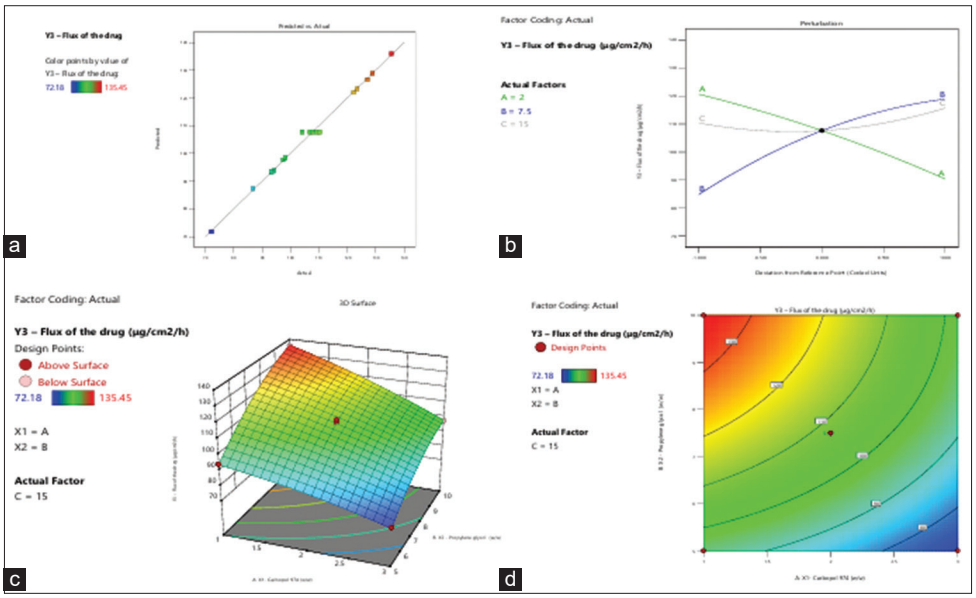

Fig. 5: (a) Predicted versus actual values of the response flux of the drug (b) Perturbation plot displaying the individual influence of variables on Y3 (c and d) 3-D response surface methodology and contour plot displaying the interactive influence of A and B on Y3

exceeds the ideal threshold of 4, indicating that the model is robust enough to guide design space exploration. The perturbation plot in Fig. 5b reveals how each variable affects Y3. The equation shows that B and C have a positive effect on Y3, while A has a negative impact. At higher levels, B and C have a quadratic effect on Y3. Three-dimensional response surface and contour plots in Fig. 5c and d demonstrate the interactive influence of variables A and B.

Numerical optimization, applying desirable constraints, identified the optimal levels for the critical process parameters (Carbopol 974 [A: X1], Propylene glycol [B: X2], and Ethanol [C: X3]) that influence gel pH (Y1), viscosity (Y2), and drug flux (Y3). The overlay plot in Fig. 6 illustrates the design space for the variables and responses, optimized with a desirability value of 1.000. To ensure accuracy, chromatographic conditions were selected as a control method for the design-space plot. The optimization process yielded successful results with Carbopol 974 (2.327 w/w), Propylene glycol (6.096), and Ethanol (10.618). The optimization procedure was validated by conducting three tests under the optimal critical variable levels. Drug-loaded NS-based hydrogel formulations were prepared under these ideal conditions and subsequently tested.

Carbopol gel formulations containing 1% w/w VO-loaded NS (VONS3, VONS7, and VONS12 gels) were prepared. All of the formulations were non-irritating, as their pH values ranged from 5.4 to 5.8, which is within the normal skin pH range. The rheological properties of the gel formulations showed viscosities ranging from 3356.65±128.76 to 3454.65±202.13 cps. Hydrogels, being hydrophilic polymers, are capable of holding large quantities of water within their three-dimensional networks. The adsorption and fusion of these gels onto the skin surface are crucial for drug penetration in NS-based hydrogel formulations. A penetration-enhancing non-ionic surfactant helps disrupt the tightly packed lipids in the stratum corneum's extracellular gaps, modifying its barrier function. These interactions between the skin and NS components may explain the observed differences in drug delivery. When NS-based hydrogel formulations fuse with the skin surface, they promote greater drug flow, allowing the nanocarriers to directly transfer the drug. VONS12 gel showed higher flux in the egg membrane (104.12±1.87 μg cm^{-2} h^{-1}), while VONS8 gel exhibited greater flux in rat skin (123.12±2.65 μg cm^{-2} h^{-1}).

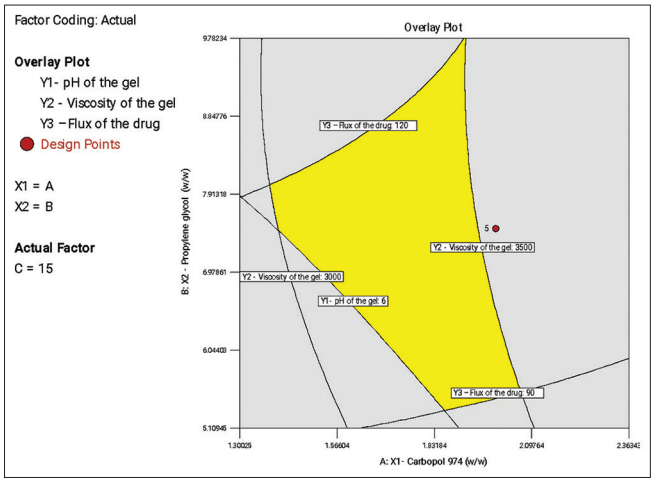

Fig. 6: Overlay plot showing the design space

In vitro, skin permeation studies were performed using vertical Franz diffusion cells at 37°C to evaluate the effect of NS encapsulation on VO penetration and skin deposition. Three NS-encapsulated VO gel formulations and a carbopol gel control were tested. These formulations included Control (free VO gel), Test 1 (VONS2), Test 2 (VONS8), and Test 3 (VONS12). To assess transdermal VO administration, receptor media were sampled at 0.5, 1, 2, 4, 6, 8, 10, and 12 h (Fig. 7). After 12 h of application, neither the control nor the test formulations showed any VO in the receptor phase, indicating that no transdermal delivery occurred. The studies also included measurements of VO in the stratum corneum and epidermis/dermis of rat skin after the 12-h permeation test.

VO skin penetration significantly improved 12 h after treatment with all test formulations compared to the control group. At the 12-h mark, the cumulative VO levels in the gel formulations (Control, Test 1, Test 2, Test 3) were 5.34±0.43, 41.23±1.83, 45.32±2.21, and 55.38±2.05 μg/cm^2, respectively. This indicates that the gel formulations with encapsulated VO allowed for more than 10–12 times greater skin penetration than the gel containing free VO. Among the test formulations, VONS12 gel exhibited the highest VO skin penetration at the 12-h mark, outperforming both VONS2 and VONS8 gels. Test 3 resulted in 1.3 times more VO delivery through the skin compared to Test 1 and Test 2. The distribution of VO in excised rat skin is shown in Fig. 7a and b.

In the *in vitro* skin penetration study, a notable increase in VO concentration in the stratum corneum (SC) was observed at 3, 6, 9, and 12 h post-application of the NS formulation ($p<0.05$). Similarly, the concentration of VO in the epidermis/dermis ([E+D]) also significantly increased at the same time points ($p<0.05$). The enhanced VO permeability and deposition were attributed to NS encapsulation and the penetration-enhancing properties of the Carbopol gel.

In addition, the antibacterial properties of VO were tested against A. fumigatus and C. albicans using agar diffusion microbiological assays. NS-based VO gels demonstrated inhibitory effects on the growth of C. albicans and A. fumigatus, unlike the VO gel alone. After 24 h, the inhibitory zones for NS-based VO gels indicated reduced microbial growth.

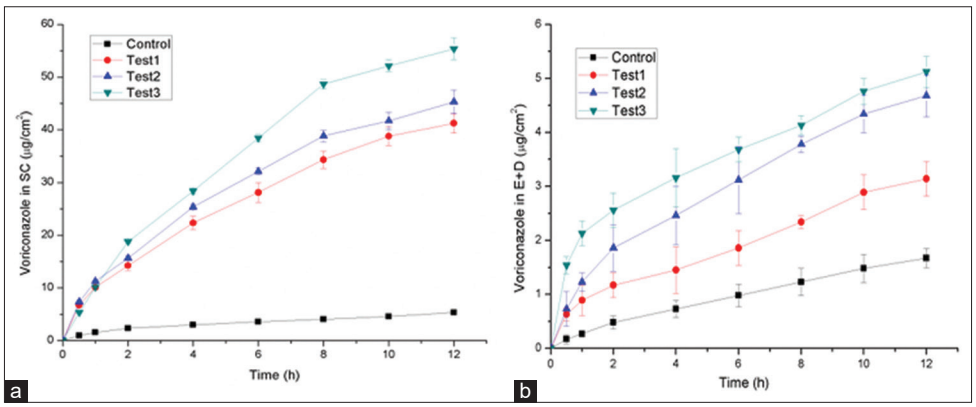

Fig. 7: The time course of *in vitro* skin permeation of PO incorporated into gel formulations in (a) Stratum corneum and (b) Epidermis and dermis. (All the results are expressed as mean±standard deviation of triplicate experiments)

Finally, the gel formulations maintained their pH and clarity at room temperature. The stability studies revealed that the VO gel degraded by 16% over a period of 3 months, while the VONS gel formulations did not experience any loss of VO during the same timeframe. This durability is attributed to the stability provided by CDNS.

CONCLUSION

This study developed, characterized, and assessed a VO hydrogel formulation incorporating CDNS. The hydrophilic properties of hydrogels enabled them to retain large amounts of water within their three-dimensional structures. The adsorption and integration of NS onto the skin surface facilitated enhanced VO penetration. A non-ionic surfactant with penetration-enhancing properties disrupted the stratum corneum's tightly packed lipids in the extracellular spaces, altering its barrier function. Changes observed in VO flow across membranes and excised skin indicated modifications to the skin barrier. The association and fusion of NS with the skin surface increased flow, enabling direct drug delivery through nanocarriers. The findings suggest that NS-based hydrogel formulations can significantly enhance the transdermal delivery of VO, offering potential improvements for drug delivery systems.

ETHICS APPROVAL AND CONSENT TO PARTICIPATE

With approval of IAEC no: 1447/PO/Re/S/11/CPCSEA-96/A.

CONSENT FOR PUBLICATION

This work is original and not published or under consideration in any other journal.

AVAILABILITY OF DATA AND MATERIAL

Will be made available on request.

ACKNOWLEDGMENTS

Not applicable.

AUTHOR'S CONTRIBUTIONS

Md Apsar Pasha carried out the entire research and prepared the manuscript. Seema Tomar and Kiran Kumar Ywere involved in the analysis of the entire data and guided and reviewed the project from time to time.

COMPETING INTERESTS

The authors declare that they have no competing interests.

FUNDING

We have not received any funding.

REFERENCES

1. Prajapati M, Shende S, Jain V, Gupta A, Kumar Goyal M. Formulation and *in vitro* percutaneous permeation and skin accumulation of voriconazole microemulsified hydrogel. Asian J Pharm Technol. 2021 Oct-Dec;11(4):267-72. doi: 10.52711/2231-5713.2021.00044
2. Teixeira MM, Carvalho DT, Sousa E, Pinto E. New antifungal agents with azole moieties. Pharmaceuticals (Basel). 2022 Nov;15(11):1427. doi: 10.3390/ph15111427, PMID 36422557
3. Pemán J, Salavert M, Cantón E, Jarque I, Romá E, Zaragoza R, *et al*. Voriconazole in the management of nosocomial invasive fungal infections. Ther Clin Risk Manag. 2006 Jun;2(2):129-58. doi: 10.2147/tcrm.2006.2.2.129, PMID 18360588
4. Veringa A, Geling SF, Span LF, Vermeulen KM, Zijlstra JG, Van Der Werf TS, *et al*. Bioavailability of voriconazole in hospitalised patients. Int J Antimicrob Agents. 2017 Feb;49(2):243-6. doi: 10.1016/j.ijantimicag.2016.10.010, PMID 28012684
5. Purkins L, Wood N, Kleinermans D, Greenhalgh K, Nichols D. Effect of food on the pharmacokinetics of multiple-dose oral voriconazole. Br J Clin Pharmacol. 2003 Jul;56(1) Suppl 1:17-23. doi: 10.1046/j.1365-2125.2003.01994.x, PMID 14616409
6. Demir SÖ, Atici S, Akkoç G, Yakut N, İkizoğlu NB, Eralp EE, *et al*. Neurologic adverse events associated with voriconazole therapy: Report of two pediatric cases. Case Rep Infect Dis. 2016 Dec;2016:3989070. doi: 10.1155/2016/3989070, PMID 27313918
7. Pahuja P, Kashyap H, Pawar P. Design and evaluation of HP-β-CD based voriconazole formulations for ocular drug delivery. Curr Drug Deliv. 2014 Apr;11(2):223-32. doi: 10.2174/15672018106661312241005205, PMID 24365062
8. De Almeida Campos L, Fin MT, Santos KS, De Lima Gualque MW, Freire Cabral AK, Khalil NM, *et al*. Nanotechnology-based approaches for voriconazole delivery applied to invasive fungal infections. Pharmaceutics. 2023 Jan;15(1):266. doi: 10.3390/pharmaceutics15010266, PMID 36678893
9. Kaur A, Dubey G, Sharma N, Pant R, Bharatam PV, Tikoo K, *et al*. High dose nanocrystalline solid dispersion powder of voriconazole for inhalation. Int J Pharm. 2022 Nov;622:121827. doi: 10.1016/j.ijpharm.2022.121827, PMID 35589006
10. Anil L, Mohandas S. *In vitro* antioxidant and anticancer activity of *Macranga peltata* leaf extracts on lung cancer cell lines. Int J Curr Pharm Res. 2023 Apr;15(4):26-32. doi: 10.22159/ijcpr.2023v15i4.3019
11. Edis Z, Wang J, Waqas MK, Ijaz M, Ijaz M. Nanocarriers-mediated drug delivery systems for anticancer agents: An overview and perspectives. Int J Nanomedicine. 2021 Apr;16:1313-30. doi: 10.2147/IJN.S289443, PMID 33628022
12. Conceicao J, Adeoye O, Cabral-Marques HM, Lobo JM. Cyclodextrins as drug carriers in pharmaceutical technology: The state of the art. Curr Pharm Des. 2018 May;24(13):1405-33. doi: 10.2174/1381612824666171218125431, PMID 29256342
13. Reddy KS, Bhikshapathi D, Kumar JP. Unlocking dabrafenib's potential: A quality by design (QBD) journey to enhance permeation and oral bioavailability through nanosponge formulation. Braz J Pharm Sci. 2025;61:e24209. doi: 10.1590/s2175-97902025e24209
14. Rao MR, Chaudhari J, Trotta F, Caldera F. Investigation of cyclodextrin-based nanosponges for solubility and bioavailability enhancement of rilpivirine. AAPS PharmSciTech. 2018 Dec;19(5):2358-69. doi: 10.1208/s12249-018-1064-6, PMID 29869305
15. Kumar S, Dalal P, Rao R. Cyclodextrin nanosponges: A promising approach for modulating drug delivery. In: Colloid Science Pharmceutical Nanotechnology. Germany: BoD - Books on Demand; 2020 Jan. p. 79.
16. Krabicová I, Appleton SL, Tannous M, Hoti G, Caldera F, Rubin Pedrazzo A, *et al*. History of cyclodextrin nanosponges. Polymers. 2020 May;12(5):1122. doi: 10.3390/polym12051122, PMID 32423091
17. Desai D, Shende P. Drug-free cyclodextrin-based nanosponges for antimicrobial activity. J Pharm Innov. 2021 Aug;16(2):258-68. doi: 10.1007/s12247-020-09442-4
18. Vakilinezhad MA, Tanha S, Montaseri H, Dinarvand R, Azadi A, Akbari Javar H. Application of response surface method for preparation, optimization, and characterization of nicotinamide loaded solid lipid nanoparticles. Adv Pharm Bull. 2018 Jun;8(2):245-56. doi: 10.15171/apb.2018.029, PMID 30023326
19. Priyanka K, Sahu PL, Singh S. Optimization of processing parameters for the development of *Ficus religiosa* L. extract loaded solid lipid nanoparticles using central composite design and evaluation of antidiabetic efficacy. J Drug Deliv Sci Technol. 2018 Jan;43:94-102. doi: 10.1016/j.jddst.2017.08.006
20. Nekkaa A, Benaissa A, Lalaouna AE, Mutelet F, Canabady-Rochelle L. Optimization of the extraction process of bioactive compounds from *Rhamnus alaternus* Leaves using Box-Behnken experimental design. J Appl Res Med Aromat Plants. 2021 Jul;25:100345. doi: 10.1016/j.jarmap.2021.100345
21. Ahmad A, Rehman MU, Wali AF, El-Serehy HA, Al-Misned FA, Maodaa SN, *et al*. Box-Behnken response surface design of polysaccharide extraction from *Rhododendron arboreum* and the evaluation of its antioxidant potential. Molecules. 2020 Aug;25(17):3835. doi: 10.3390/molecules25173835, PMID 32846866
22. Sarfaraz MD, Mehboob SZ, Doddayya H. Preparation and characterization of fluconazole topical nanosponge hydrogel. Int J Pharm Pharm Sci. 2024 Apr;16(4):18-26.
23. Viswaja M, Bhikshapathi DV, Palanati M, Babu AK, Goje A. Formulation and evaluation of ibrutinib nanosponges incoporated tablet. Int J Appl Pharm. 2023 Feb;15(2):92-7. doi: 10.22159/ijap.2023v15i2.46813
24. Anusha R, Mothilal M. Development of nanosponges-based topical formulation for the effective delivery of selected antifungal drug. Int J Appl Pharm. 2024 May;16(5):146-55. doi: 10.22159/ijap.2024v16i5.51466

25. Ghurghure SM, Jadhav T, Kale S, Phatak AA. Formulation and evaluation of posaconazole loaded nanostructured lipid carriers for topical drug delivery system. Curr Trends Pharm Pharm Chem. 2022 Sep;4(3):126-34. doi: 10.18231/j.ctppc.2022.022
26. Swaminathan S, Vavia PR, Trotta F, Torne S. Formulation of β-cyclodextrin based nanosponges of itraconazole. J Incl Phenom Macrocycl Chem. 2007 Apr;57(1-4):89-94. doi: 10.1007/s10847-006-9216-9
27. Milanowski B, Wosicka-Frąckowiak H, Główka E, Sosnowska M, Woźny S, Stachowiak F, *et al*. Optimization and evaluation of the *in vitro* permeation parameters of topical products with non-steroidal anti-inflammatory drugs through Strat-M® membrane. Pharmaceutics. 2021 Aug;13(8):1305. doi: 10.3390/pharmaceutics13081305, PMID 34452264
28. Hummer J, Birngruber T, Sinner F, Page L, Toner F, Roper CS, *et al*. Optimization of topical formulations using a combination of *in vitro* methods to quantify the transdermal passive diffusion of drugs. Int J Pharm. 2022 Apr;620:121737. doi: 10.1016/j.ijpharm.2022.121737, PMID 35413396